Molecular Therapy
Methods & Clinical Development
Original Article

Nonclinical Safety Evaluation of scAAV8-*RLBP1* for Treatment of *RLBP1* Retinitis Pigmentosa

Timothy K. MacLachlan,[1] Mark N. Milton,[2] Oliver Turner,[3] Francis Tukov,[3] Vivian W. Choi,[4,7] Jan Penraat,[3,8] Marie-Hélène Delmotte,[5,9] Lydia Michaut,[6] Bruce D. Jaffee,[4] and Chad E. Bigelow[4]

[1]Preclinical Safety, Novartis Institutes for BioMedical Research, Cambridge, MA, USA; [2]Pharmacokinetic Sciences, Novartis Institutes for BioMedical Research, Cambridge, MA, USA; [3]Preclinical Safety, Novartis Institutes for BioMedical Research, East Hanover, NJ, USA; [4]Ophthalmology Research, Novartis Institutes for BioMedical Research, Cambridge, MA, USA; [5]Preclinical Safety, Novartis Institutes for BioMedical Research, Basel, Switzerland; [6]Pharmacokinetic Sciences, Novartis Institutes for BioMedical Research, Basel, Switzerland

Retinitis pigmentosa is a form of retinal degeneration usually caused by genetic mutations affecting key functional proteins. We have previously demonstrated efficacy in a mouse model of *RLBP1* deficiency with a self-complementary AAV8 vector carrying the gene for human *RLBP1* under control of a short *RLBP1* promoter (CPK850).[1] In this article, we describe the nonclinical safety profile of this construct as well as updated efficacy data in the intended clinical formulation. In *Rlbp1*$^{-/-}$ mice dosed at a range of CPK850 levels, a minimum efficacious dose of 3 × 10^7 vg in a volume of 1 μL was observed. For safety assessment in these and *Rlbp1*$^{+/+}$ mice, optical coherence tomography (OCT) and histopathological analysis indicated retinal thinning that appeared to be dose-dependent for both *Rlbp1* genotypes, with no qualitative difference noted between *Rlbp1*$^{+/+}$ and *Rlbp1*$^{-/-}$ mice. In a non-human primate study, *RLBP1* mRNA expression was detected and dose dependent intraocular inflammation and retinal thinning were observed. Inflammation resolved slowly over time and did not appear to be exacerbated in the presence of anti-AAV8 antibodies. Biodistribution was evaluated in rats and satellite animals in the non-human primate study. The vector was largely detected in ocular tissues and low levels in the optic nerve, superior colliculus, and lateral geniculate nucleus, with limited distribution outside of these tissues. These data suggest that an initial subretinal dose of ~3 × 10^7 vg/μL CPK850 can safely be used in clinical trials.

INTRODUCTION

Genetic forms of blindness, such as retinitis pigmentosa (RP), offer opportunities for gene delivery treatment given the monogenic nature in subsets of patients.[2] A population of RP patients carry recessive null mutations in the retinaldehyde binding protein 1 (*RLBP1*) gene that encodes cellular retinaldehyde-binding protein (CRALBP).[3–6] CRALBP is expressed in the retina in retinal pigment epithelium (RPE) and Müller cells. It binds 11-cis-retinol and 11-cis-retinal in support of chromophore supply to rod and cone photoreceptors.[7–9]

RLBP1 RP is characterized by abnormally slow dark adaptation in youth followed by progressive vision loss owing to photoreceptor degeneration. A previous publication presented efficacy results obtained in a mouse model of CRALBP deficiency exhibiting slow dark adaptation (*Rlbp1*$^{-/-}$ mice) using a self-complementary AAV8 vector expressing the human *RLBP1* gene under transcriptional control of a short *RLBP1* promoter (CPK850).[1] Subretinal delivery of this viral vector improved the rate of dark adaptation in *Rlbp1*$^{-/-}$ mice assessed by electroretinography (ERG) for both scotopic (rod-plus-cone) and photopic (cone) vision. The effect on scotopic vision was still present 1 year post-injection.

The safety and biodistribution of subretinal injection of adeno-associated virus (AAV) vectors has been described for a handful of products, the most detailed of which are the AAV2-*RPE65* vectors for treatment of another inherited degenerative disease of the retina called Leber's congenital amaurosis (LCA).[10,11] Nonclinical safety studies of 3 months in length were performed in a dog model of LCA as well as in normal non-human primates. In both cases, observations were made of acute and temporary inflammation and moderate levels of retinal thinning. Clinically, while some patients have experienced limited thinning of the retina as detected by optical coherence tomography (OCT), these programs have shown signs of visual improvement even in the presence of these effects.[12–14] Additional studies have been performed, evaluating the potential adverse impact of immunity against the AAV capsid by first dosing one eye and then dosing the contralateral eye some months later. This approach has proven both safe and effective in treating the disease in both animals and humans.[15–17]

While there are multiple publications describing the safety of AAV serotype 2 vectors utilizing the subretinal route of administration, a

Received 20 September 2017; accepted 18 December 2017;
https://doi.org/10.1016/j.omtm.2017.12.001.

[7]Present address: Shire Pharmaceuticals, Lexington, MA, USA

[8]Present address: Alpha Omega Veterinary Services, Lafayette, NJ, USA

[9]Present address: Teva Pharmaceuticals, Basel, Switzerland

Correspondence: Timothy K. MacLachlan, Preclinical Safety, Novartis Institutes for BioMedical Research, Cambridge, MA, USA.
E-mail: timothy.maclachlan@novartis.com

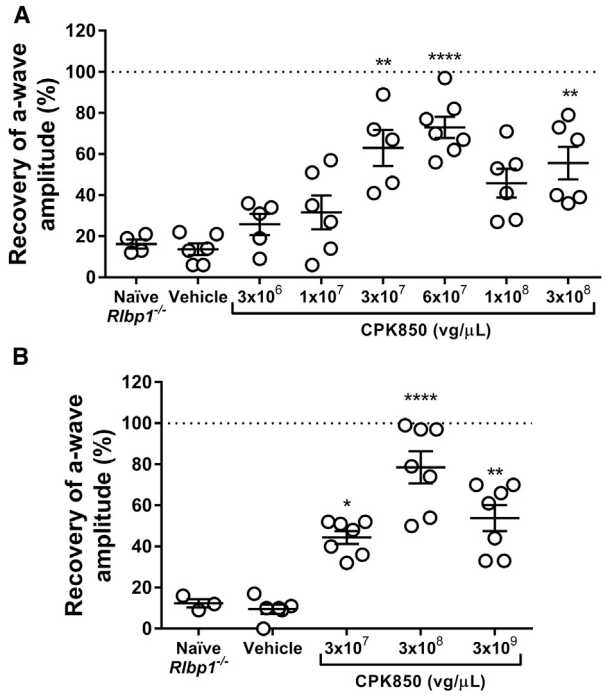

Figure 1. Efficacy of CPK850 in *Rlbp1*$^{-/-}$ Mice

(A) Dose response efficacy study evaluating the effect of increasing doses of CPK850 12 weeks post-injection. (B) Confirmation of efficacy in the *Rlbp1*$^{-/-}$ mouse safety study acquired 10–11 weeks post-injection. Note that doses delivered to mice are equivalent if expressed in vg/eye or vg/µL since the volume of injection is 1 µL/eye. Doses presented are rounded to the nearest whole number. *p ≤ 0.05, **p ≤ 0.01, ****p ≤ 0.0001 versus the naive group.

nonclinical safety package using AAV8 has not been described to date. In addition, use of a self-complementary genomic structure, which facilitates speed of expression once in the cell, is a more novel method for ocular treatment. Here we describe the nonclinical safety package for CPK850 performed in rodents and non-human primates. These studies allow us to answer questions regarding the safety of the capsid self-complementary genomic structure, exogenous *RLBP1* expression in wild-type and *Rlbp1*$^{-/-}$ genetic backgrounds, and distribution of the CPK850 DNA.

RESULTS

Efficacy of CPK850 in *Rlbp1* Knockout Mice in the Clinical Formulation

A previous publication describing vector selection and dose-dependent efficacy of CPK850 identified a minimally efficacious dose of 3×10^8 vector genomes (vg)/eye (3×10^8 vg/µL in a 1 µL dose) in *Rlbp1*$^{-/-}$ mice.[1] The research grade vector used in this earlier dose response study was formulated and diluted without addition of surfactant. Since there is potential of reduced AAV recovery from injection devices in the absence of surfactant,[18,19] studies presented in Figure 1 were performed with CPK850 formulated with 0.001% Pluronic F68. Additionally, CPK850 used for studies in Figure 1 was produced using the same process configuration as the final good manufacturing process.

Table 1. Designs of *Rlbp1*$^{-/-}$ *and Rlbp1*$^{+/+}$ Mouse Toxicology Studies

	Number of Eyes		
Group	*Rlbp1*$^{-/-}$	*Rlbp1*$^{+/+}$	Dose Concentration (vg/µL)
1	18	20	3.2×10^9
2	20	24	3.2×10^8
3	22	20	3.2×10^7
4	20	18	vehicle
5	20	30	uninjected

Results of dark adaptation measurements for CPK850 in *Rlbp1*$^{-/-}$ mice are presented in Figure 1. The minimally efficacious dose providing robust restoration of dark adaptation was approximately 3×10^7 vg/µL in the dose response study (Figure 1A). Dark adaptation (efficacy) ERG from a subset of mice in the *Rlbp1*$^{-/-}$ safety study confirmed the minimally efficacious dose of approximately 3×10^7 vg/µL and also provided indirect evidence of CRALBP expression (Figure 1B).

Safety of CPK850 in *Rlbp1* Wild-Type and Knockout Mice

A study was conducted comparing the safety of CPK850 in both *Rlbp1*$^{+/+}$ and *Rlbp1*$^{-/-}$ mice to determine if there are disease-specific toxicities induced by CPK850 (Table 1). Mice received CPK850 at doses from 3.2×10^7 to 3.2×10^9 vg/µL delivered subretinally in 1 µL. To confirm injection success and as an indirect confirmation of vector-mediated CRALBP expression, ERGs were performed 10 to 11 weeks post-injection. All dose levels achieved improved dark adaptation as measured by recovery of a-wave amplitude in *Rlbp1*$^{-/-}$ mice (Figure 1B). *Rlbp1*$^{+/+}$ mice exhibited robust ERG a-wave recovery consistent with endogenous CRALBP expression and did not exhibit changes in dark adaptation post-injection (data not shown).

ERG measurements in the mouse safety studies were designed to provide indirect confirmation of CRALBP expression in a subset of mice rather than to detect safety signals associated with CPK850 delivery. However, dark-adapted (scotopic) ERG a-wave data were provided by the dark adaptation measurements as part of baseline retinal function determination. Scotopic ERG a-wave results were unremarkable for both *Rlbp1*$^{-/-}$ (Figure S2A) and *Rlbp1*$^{+/+}$ (Figure S2B) mice, with no significant differences detected between any groups for either genotype.

OCT images were acquired from all mice reported in the study results before injection (baseline), 1 week post-injection, and 12 weeks post-injection. At 13 weeks post-injection, the animals were euthanized and eyes were evaluated histologically.

In wild-type mice, animals with eyes receiving 3.2×10^9 vg/µL exhibited retinal thinning, observed by OCT, with higher incidence

Table 2. Results of OCT Imaging Observations in *Rlbp1*$^{+/+}$ Mice 12 Weeks Post-injection

Dose Group	Dose Concentration (vg/μL)	No. of Eyes Evaluated[a]	Retina Appears Normal	Injection Site Only	Hyper-reflective Features in Retina without Thinning	Retinal Thinning with IS/OS Preservation	Retinal Thinning with Loss of IS/OS Structure	Other
1	3.2×10^9	12	0	2	1	2	6	1
2	3.2×10^8	16	6	1	1	2	5	1
3	3.2×10^7	12	3	4	0	1	3	1
4	vehicle	15	4	5	0	2	3	1
5	uninjected	28	20	0	0	0	0	8

OCT images representative of the lesions noted in this table and Table 3 are shown in Figure S1. A description of each lesion category is provided in Table S1.
[a]Some eyes that were injected were not analyzed due to failed injection, poor image quality, or animal death. "Other" indicates anomalies outside the injection site that were not consistent with more common findings observed in dosed areas.

than groups receiving vehicle, 3.2×10^7 or 3.2×10^8 vg/μL CPK850 (Table 2). A slightly increased incidence of retinal thinning was observed in *Rlbp1*$^{-/-}$ mice by OCT in the highest dose group of 3.2×10^9 vg/μL when compared to the 3.2×10^8 vg/μL dose group and at an even higher incidence compared to animals with eyes receiving 3.2×10^7 vg/μL (Table 3). However, the incidence of retinal thinning in eyes receiving vehicle was similar to that observed in the 3.2×10^9 vg/μL dose group, so a true CPK850-related effect was difficult to determine. Estimated retinal thickness measures were consistent with these observations (Figure 2).

Histologically, retinal thinning among the groups and among the mouse strains was similar to findings by OCT (Figure 3). There were no notable differences in overall retinal morphology, outer retinal morphology, or outer nuclear layer morphology between left and right eyes or male and female eyes, and there were no microscopic findings in the uninjected animals. The lesions were typically focal to locally extensive and affected up to approximately 50% of the retina, but more typically less than approximately 10%. The RPE was typically normal at these sites but was occasionally minimally hypertrophied in the more severe lesions. The incidence and severity of these abnormalities tended to increase with respect to dose level.

Data from OCT and histology qualitatively agreed with each other, suggesting the two methods for assessing the effects of subretinal CPK850 provide similar results. Overall, there did not appear to be a disease-specific pathology associated with CPK850 in mice.

Safety of CPK850 in Non-human Primates

To assess the safety of CPK850 in an eye with similar anatomy to humans, we performed a study in cynomolgus non-human primates for 6 months following injection (Table 4). Briefly, there were five groups of animals, all dosed in the right eye on study day 1 with 100 μL of vehicle or CPK850 at concentrations ranging from 3.3×10^6 to 3.3×10^9 vg/μL. At the 3-month time point, a subset of animals dosed with CPK850 (1 male and 1 female per group in groups 2–5) were sacrificed for evaluation of *RLBP1* expression and shedding and distribution of CPK850. Also at day 51 of the study, a subset of the remaining animals (2 males and 2 females per group in groups 1 and 3–5) were dosed in the contralateral (left) eye with a dose of 3.3×10^7 vg/μL CPK850 in order to determine any potential effects of antibodies against the AAV8 capsid on a subsequent injection. This dose was chosen because it yielded the least amount of inflammation between groups 3–5 and, as such, would provide a window to observe potential effects of immunogenicity-related toxicities. At the 6-month time point, all remaining animals were sacrificed for histopathological analysis of the eye and other tissues. Ocular exams including slit lamp, indirect ophthalmoscopy, OCT, intraocular pressure (IOP) and ERG were conducted at various intervals throughout the study. Blood was collected at various time points during the study to assess any

Table 3. Results of OCT Imaging Observations in *Rlbp1*$^{-/-}$ Mice 12 Weeks Post-injection

Dose Group	Dose Concentration (vg/μL)	No. of Eyes Evaluated[a]	Retina Appears Normal	Injection Site Only	Hyper-reflective Features in Retina without Thinning	Retinal Thinning with IS/OS Preservation	Retinal Thinning with Loss of IS/OS Structure	Other
1	3.2×10^9	12	3	1	2	1	5	0
2	3.2×10^8	19	4	6	1	4	4	0
3	3.2×10^7	21	9	6	0	0	4	2
4	vehicle	19	2	5	0	3	6	3
5	uninjected	18	12	0	0	0	0	6

OCT images representative of the lesions noted in this table and Table 2 are shown in Figure S1. A description of each lesion category is provided in Table S1.
[a]Some eyes that were injected were not analyzed due to failed injection, poor image quality, or animal death. "Other" indicates anomalies outside the injection site that were not consistent with more common findings observed in dosed areas.

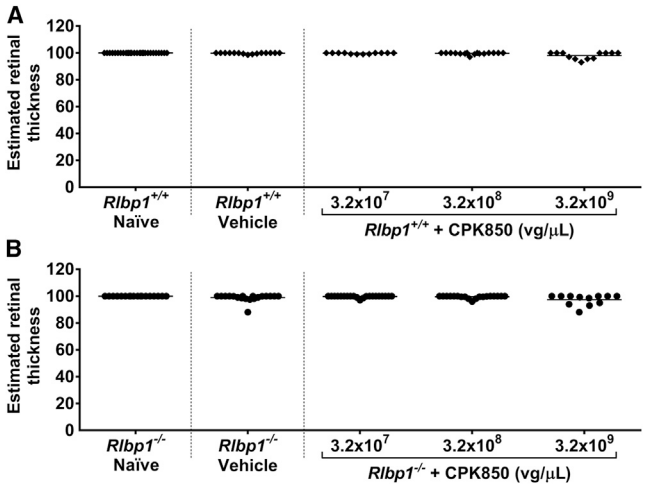

Figure 2. Estimated Retinal Thickness in *Rlbp1*$^{+/+}$ and *Rlbp1*$^{-/-}$ Mice 12 Weeks after Injection with CPK850

Estimated retinal thickness in *Rlbp1*$^{+/+}$ (A) and *Rlbp1*$^{-/-}$ (B) mice 12 weeks after injection with CPK850. OCT images were aquired from mice dosed with CPK850 and evaluated for retinal thickness based on the equation provided in the Materials and Methods. Note that doses delivered to mice are equivalent if expressed in vg/eye or vg/μL since the volume of injection is 1 μL/eye.

potential systemic toxicity and humoral immunity against AAV8. Finally, excreta (tears, throat swabs, urine, and feces) and tissues (eye, brain, and lacrimal gland) were collected for shedding and distribution analysis, which is described below in the Biodistribution and Expression Analysis section.

In the cohort of animals intended to evaluate expression of *RLBP1*, expression was measured via qRT-PCR methods that differentiated the endogenous non-human primate *RLBP1* expression from the exogenous human *RLBP1* expression from CPK850. Punches were made in the retina in the approximate region of subretinal injection in the dosed right eye (Figure 4) and a similar location in the undosed left eye, and the samples were processed to prepare RNA. While endogenous levels of expression were noted across all animals, no human *RLBP1* RNA was detected in the undosed left eye and a dose-related increase in expression was noted in the dosed right eyes.

Dose levels of 3.3×10^6 and 3.3×10^7 vg/μL were well-tolerated with minimal levels of transient intraocular inflammation, consistent or slightly higher than that observed in the vehicle control, and findings on OCT and ERG were consistent with control. Dose levels of 3.3×10^8 and 3.3×10^9 vg/μL were associated with progressively higher levels of intraocular inflammation, thinning of the outer nuclear layer, and reductions in ERG signals. Representative scotopic and photopic ERGs from animals in each group at the week 8 and 24 time points are shown in Figure 5. Group 5 animals were observed to have mildly reduced scotopic and photopic ERGs at week 8, but the signal in the dosed eye largely recovered by week 24. Significant inflammation at the week 8 time point may have inhibited light from reaching the retina and, when that inflammation resolved by week 24, a more normal ERG reading was obtained. Inflammation at all dose levels progressively recovered over the course of the study; however, at the higher dose levels, some findings persisted until the terminal sacrifice (Figures 6 and 7).

All animals in the CPK850 dosed groups showed the generation of treatment-induced or treatment-boosted anti-AAV8 antibodies over the course of the study with the exception of two animals dosed with 3.3×10^7 vg/μL (Table 5). As described above, at day 51 of the study, CPK850 was dosed into the contralateral eye of a subset of animals. A dose of 3.3×10^7 vg/μL was chosen because it resulted in some initial inflammation upon dosing into the right eye. In this subset of animals, no findings of inflammation were observed in those eyes that were more severe than the right eyes having initially received 3.3×10^7 vg/μL, suggesting that the generation of anti-AAV8 antibodies from the initial injection did not create any new toxicities and did not enhance the inflammation observed with the initial dose (Figure 7).

One animal displayed a very transient antibody response to CRALBP in the low-dose group late in the study (data not shown). There was no more significant inflammation or histological findings in this animal compared to others in the cohort.

Histopathological analysis of the eyes both at 3 and 6 months post-dose showed varying levels of retinal atrophy/degeneration, choroidal mononuclear cell infiltrates, and pigmented cells in the subretinal space, particularly in animals receiving doses $\geq 3.3 \times 10^8$ vg/μL (Figure 8). Retinal atrophy/degeneration was characterized by single, locally extensive, or multiple foci of thinning and/or disorganization of the retina. This change predominantly affected the photoreceptor and outer nuclear layers but occasionally extended the full thickness of the retina. Based on the ophthalmic and microscopic findings observed among animals given 3.3×10^8 or 3.3×10^9 vg/μL to the right eye and the extent of recovery over time, the no observed adverse effect level (NOAEL) was considered to be 3.3×10^7 vg/μL.

Distribution and Shedding of CPK850 after Subretinal Injection in Rats and Non-human Primates

Male and female brown Norway rats were dosed with 3.3×10^9 vg/μL or the same volume of vehicle to evaluate biodistribution. Rats were used for this comprehensive evaluation for biodistribution because more animals could be used to understand consistency in low level measurements. Blood and selected tissues were collected on study day 15 (i.e., 2 weeks post-dose) from five animals/sex in the vehicle dose group and five animals/sex/time point in the CPK850 dose group on study days 15, 57, and 85 (Tables 6 and 7). To assess viral shedding, nasopharyngeal swabs were collected on study day 15 from animals scheduled for sacrifice. Urine and feces were collected on study day 8 from animals scheduled to be sacrificed on study day 15.

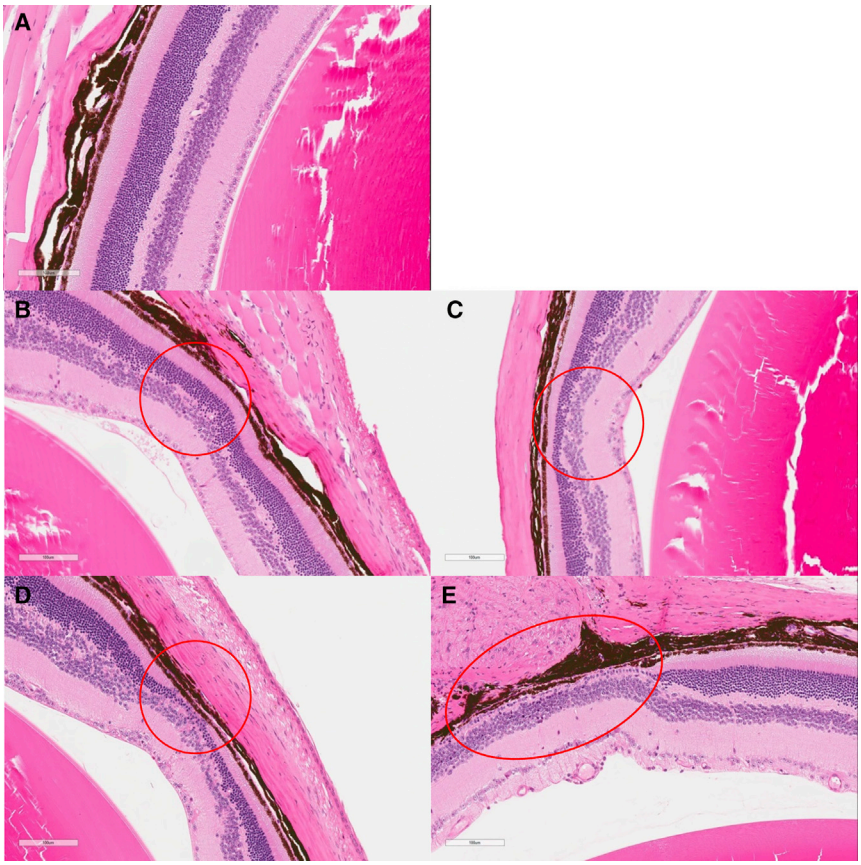

Figure 3. Representative Photomicrographs of the Four Histopathological Lesion Grades for Atrophy (Thinning) of the Outer Retina in *Rlbp1*$^{-/-}$ Mice (Depicted within the Red Circles)

Mice from (A) control-graded as "normal". (B) Vehicle group graded as "minimal". (C) Vehicle group graded as "mild". (D) 3.2×10^8 vg/μL group graded as "moderate". (E) 3.2×10^9 vg/μL group graded as "marked"; the lesion extends beyond the edge of the panel (scale bar, 100 μm, H&E).

The tissues and matrices were analyzed using a PCR assay with a limit of detection of 10 copies/μg DNA and a limit of quantitation of 50 copies/μg DNA. CPK850 was detected in the dosed right eye, optic nerve (right eye), mandibular lymph nodes (right side), spleen, and liver. CPK850 persisted at similar levels in the dosed eye throughout the study, whereas the amount of CPK850 in the optic nerve (dosed eye) decreased over time. CPK850 was also detected in the liver and spleen, with the concentrations of vector in these tissues decreasing with time. CPK850 was not detected in the gonads (ovary and testes) or excreta and nasopharyngeal swabs. A detailed description of the distribution in each tissue is provided in Table 8.

A limited panel of tissues was examined in non-human primates for distribution of CPK850 (Table 9). Tissues connected to or adjacent to the eyes were taken during week 13 post-dose from one male and one female animal of each dose group. CPK850 was not detected in any tissues collected from animals dosed with 3.3×10^6 vg/μL. At doses $\geq 3.3 \times 10^7$ vg/μL, CPK850 was detected in the optic nerve, optic chiasm, and optic tract of the right (dosed) eye of all 6 animals, with the concentrations tending to increase as the dose increased. CPK850 was not detected in the optic nerve of the left eye, but it was detected in the optic chiasm and optic tract of the left side, with the concentrations of CPK850 being lower than that observed in the corresponding tissues collected from the right side. CPK850 was detected in the right and left lacrimal gland in one animal and in the right lacrimal gland of 3 additional animals. CPK850 was detected in both the left and right lateral geniculate nucleus of two out of 6 animals. In the superior colliculus, CPK850 could be detected in the tissue collected from the right side (2 animals) and left side (5 animals). CPK850 was not detected in the visual cortex of any animal. An assessment of the tissue distribution and the excretion of CPK850 was also performed in a subset of animals (1 male and 1 female per CPK850 dosing group) in the non-human primate toxicology study. Tear samples (from left and right eyes), throat swabs, and urine and fecal swabs were collected from a selected group of animals during weeks 1, 4, 8, and 12 post-dose. Ocular tissue samples (including retina, choroid, and sclera), brain samples (including optic chiasm, optic tract, lateral geniculate nucleus, visual cortex, and superior colliculus), and lacrimal glands were collected. CPK850 was detected in 18 (14%) of the 128 shedding samples, which consisted of urine, tears, throat swabs, and fecal swabs (Table 10). CPK850 levels in the urine and fecal samples were below the limit of quantitation (50 copies per μg DNA) at all time points, with the exception of low levels (<200 copies) at week 1 in animals dosed with 3.3×10^8 vg/μL (1/2 in urine, 0/2 in feces) or 3.3×10^9 vg/μL (0/2 in urine, 2/2 in feces). The highest levels were detected in the tears and were detected in 8 of 32 samples, but only four of these were quantifiable, and it is uncertain if they were from the right or left eye since the tear samples from the right and left eye were combined. At 12 weeks post-dose, shedding of CPK850 was detected only in the tears of three animals and not in the urine, throat swabs, or fecal swabs from any animal.

DISCUSSION

In the last few years, several nonclinical and clinical programs have aimed to treat various genetic forms of inherited retinal dystrophy. The most advanced and well known are those that replace the *RPE65* gene, which is found mutant in LCA. In this case, AAV2 vectors have been used as a delivery mechanism because RPE cells are efficiently transduced by this serotype. The safety profile of this therapy has been described from the three independent trials that are

Table 4. Design of Non-human Primate Toxicology Study

	Animals[a]		Dose Concentration (vg/μL)[b]	
Group	Male	Female	Right Eye	Left Eye
1	4	4	0 (vehicle)	NA
2	1	1	3.3×10^6	NA
3	5	5	3.3×10^7	3.3×10^7
4	5	5	3.3×10^8	3.3×10^7
5	5	5	3.3×10^9	3.3×10^7

[a]1 male/1 female in groups 2–5 were sacrificed 3 months after dosing, and eyes were harvested for expression analysis; 2 males/2 females in groups 1 and 3–5 were sacrificed 3 months after dosing for histopathological analysis; 2 males/2 females in groups 3–5 were given a dose of CPK850 in the left eye 51 days after dosing into the right eye, and these animals, with 2 males/2 females from group 1, were sacrificed 6 months after the initial injection in the right eye.
[b]Dose volume per eye was 100 μL.

ongoing.[12–14] Nonclinically, the vector was found to induce a mild level of transient inflammation and slightly reduce the thickness of the outer nuclear layer of photoreceptors in both non-human primates as well as a canine model of LCA.[10,11]

As was described in the nonclinical program for AAV2-RPE65, the primary safety findings from this study were observations of transient ocular inflammation in non-human primate and thinning of the retina in both primates and mice. Inflammatory effects have been described from the subretinal injection procedure alone in primates as well as vitrectomy in humans. Nork et al.[20] described a study where a dose of balanced salt solution was placed subretinally into non-human primates to evaluate the general effects from retinal displacement. Mild inflammation was observed in the aqueous and vitreous humor beginning 2 days post-dose, with no signs of inflammation by 92 days post-injection.

Clinically, in the AAV-RPE65 trials, Cideciyan et al.[12] (where a maximal dose of 1 mL of 1×10^8 vg/μL was used) described no intraocular inflammation but some conjunctival inflammation over the first 2 months after dosing. Bainbridge et al.[14] described significant anterior and posterior inflammation in patients receiving a 1 mL dose of 1×10^9 vg/μL, which, in one patient, temporarily attenuated improvements to retinal sensitivity. These findings are likely secondary to the dose of the AAV vectors, as in the third trial, led by Maguire et al.,[13] where the maximum dose reported in any phase of the trial has been a 300 μL dose of 5×10^8 vg/μL, where no ocular inflammation has been reported.

In the nonclinical reports of AAV2-RPE65 safety, Jacobson et al.[10,11] have described studies of AAV2-RPE65 dosed into both dogs and non-human primates. In the dog study, where doses of 150 μL material at concentrations ranging from 1×10^6 to 3×10^{10} vg/μL were dosed subretinally, mild procedural-related inflammation was observed in all groups including control, with a few animals displaying moderate and longer lasting inflammation at the higher dose groups. Similar findings were observed in the non-human primate study, where only the concentrations of 1×10^6 and 3×10^{10} vg/μL were used, but the inflammation was rated maximally as "mild" and lasted for only 1 month post-dose.

A recent report of two new AAV serotypes, AAV7m8 and AAV8B, reported the safety after intravitreal and subretinal dosing into non-human primates at a range of 150 μL doses up to 6.6×10^9 vg/μL.[21] While the AAV8B vector did not induce any inflammation at any dose level, administration of AAV7m8 led to significant ocular inflammation, particularly at the top dose level. Similar to our set of experiments described here, Ye et al.[22,23] have described an AAV2 variant, called AAV2tYF, expressing CNBG3 in safety evaluations in both mouse and non-human primate and have also found dose-related inflammation in non-human primates up to doses of 4×10^9 vg/μL. In these studies, effects on the retina were observed, but, contrary to our findings here, these were not detected histologically, but rather by temporarily reduced rod responses on ERG. Deng et al.[24] have described the safety profile of an AAV5 vector expressing the RPGR protein in mice and found photoreceptor death at the high dose of 1.5×10^{10} vg/μL. Thus, it is possible that different serotypes, perhaps affected by different preparations of vectors, will lead to differing effects on inflammation and, ultimately, the retina.

In this study, we observed very similar effects on retinal thinning and ocular inflammation compared to those reported for other AAV-based subretinal therapies. Distribution of CPK850 also appeared to be similar to other reports for subretinal AAVs. Jacobson et al.[10,11] described distribution of AAV2-RPE65 in dogs, non-human primates, and rats. Depending on the dose and the species, vector sequences were observed temporarily in locations outside the dosed eye, such as optic chiasm, optic nerve, mandibular lymph nodes, and the lateral geniculate nucleus, all areas consistent with movement of small amounts of vector from the subretinal space to areas involved in vision or lymph drainage. In addition, we performed a nonclinical vector shedding analysis, which, to our knowledge, has not been performed previously for a subretinally administered AAV vector. While some detectable levels of CPK850 were found in tears isolated from the non-human primate study, no vector was observed in any other matrices from rat or non-human primate, including nasopharyngeal swabs, urine, and feces. Another subretinal program, RetinoStat, which utilizes an equine infectious anemia virus (EIAV) vector, also performed this analysis in nonclinical evaluations and found similar results.[25]

In conclusion, the safety profile of CPK850 appears to be consistent with other subretinally administered viral therapies. While some adverse effects were observed in the mouse and non-human primate studies described here, inflammation observed in the non-human primate was reversible and any effects on the retina did not appear to be detrimental to the long-term vision of the animal. As for the mechanism underlying retinal degeneration observed at the high doses here, we hypothesize that it could arise from overexpression of CRALBP in some cells, direct toxicity of AAV8 vector on a per cell basis, an inflammatory component shortly after injection, or these factors in combination. An effect of transgene expression level on

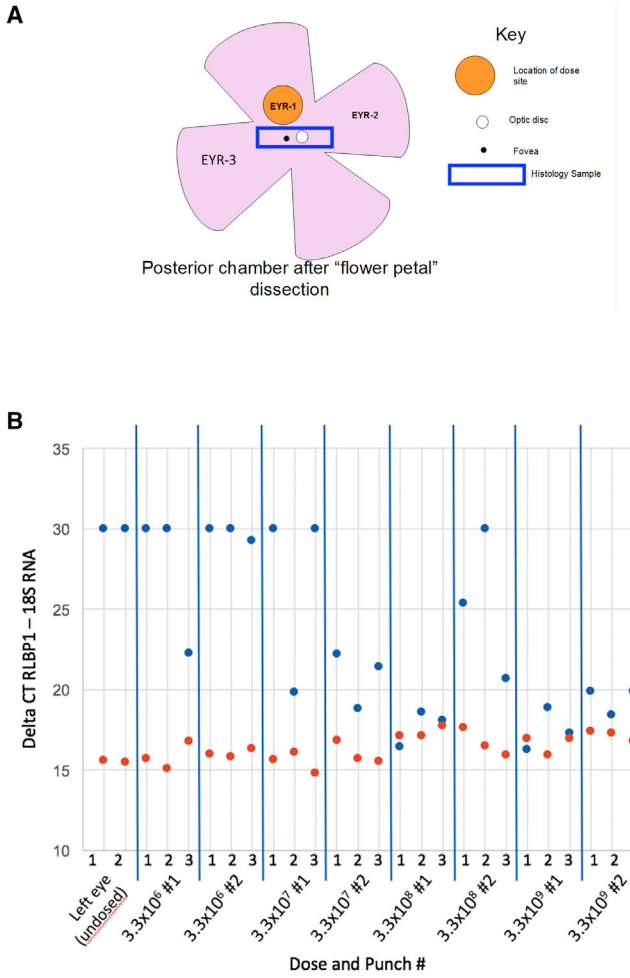

Figure 4. Expression of h*RLBP1* in the Non-human Primate Toxicology Study

Two animals per group in groups 2–5 were sacrificed at 3 months post-injection, and samples of retina were taken from the dosed (left) and undosed (right) eyes (A). Samples were processed for RNA and evaluated by RT-PCR for both non-human primate and human *RLBP1* transcript level (B). Lower Ct levels indicate higher levels of mRNA detected. The x axis in (B) indicates the "EYR" region sampled indicated in (A). A rectangular histology sample was also collected, which included the optic disc and fovea.

photoreceptor health has been previously described by Tan et al.[26] To our knowledge, this effect on the retina in nonclinical species has yet to be deconvoluted and could be done in follow-up experiments using null AAV8 vectors. In addition, in the presence of an induced systemic immune response against the AAV8 vector, a dose of CPK850 to the contralateral eye led to no safety events that were more severe than those observed with the initial dose. Finally, the minimally efficacious dose concentration of CPK850 produced using the same process configuration as the final good manufacturing process, when diluted in the clinical formulation buffer containing Pluronic F68, is equivalent to the dose concentrations found to be safe in the mouse and non-human primate safety studies described here. These data suggest, combined with our previous reports of convincing efficacy in an animal model of this syndrome, that clinical trials with CPK850 can safely be conducted.

MATERIALS AND METHODS

Animal Injections

For mouse studies, all procedures and housing conditions were approved and performed as described in the associated Novartis Cambridge Institutional Animal Care and Use Committee protocol. Injections were performed in female and male *Rlbp1*$^{-/-}$ and *Rlbp1*$^{+/+}$ mice that were acquired from Taconic Biosciences (Germantown, NY). Mice were homozygous for the Met-450 variant of RPE65.[27] The mice were on a mixed *Crb1*^{rd8} background so that wild-type, heterozygous, and *Crb1*^{rd8} homozygous mutant mice were present in all groups.[28] Mice were 12–16 weeks old at the time of injection for the dose-response efficacy study and 17–25 weeks of age for the safety studies. CPK850 or vehicle was delivered subretinally to both eyes. Pupils were first dilated through topical application of 1% cyclopentolate and 2.5%–10% phenylephrine. Mice were subsequently anesthetized with an intraperitoneal injection of ketamine/xylazine cocktail (100–150/5–10 mg/kg), and 0.5% proparacaine (topical anesthetic) was applied to the eyes. An approximately 0.5 mm incision was made nasally, posterior to the limbus, with a microscalpel. A blunt-ended needle on a 10 µL Hamilton syringe was inserted tangentially through the scleral incision toward the temporal retina until resistance was felt. 1 µL of diluted vector (containing 200 µg/mL sodium fluorescein solution) was then injected slowly into the subretinal space. For the dose response efficacy study in Figure 1A, mice received 2.9×10^6, 1.0×10^7, 2.9×10^7, 5.9×10^7, 1.0×10^8, or 2.9×10^8 vg/µL. Doses for the mouse toxicology studies are provided in Table 1. Success of the subretinal injection was confirmed by visualization of the fluorescein-containing bleb at the time of injection in combination with an OCT screen of the eyes approximately 1 week post-injection.

For non-human primate studies, the protocol was approved by the Covance Institutional Animal Care and Use Committee, and the study was conducted in compliance with all regulatory requirements. A DORC disposable dual-bore injection needle (23-gauge) was introduced directly through the sclera in the superior temporal quadrant of the globe approximately 2.5 mm posterior to the corneal limbus and moved through the vitreous under visual control using a surgical microscope viewing through a dilated pupil. The 41-gauge cannula tip was advanced from the 23-gauge needle until it gently touched the surface of the retina. The dose (100 µL per eye) was injected through

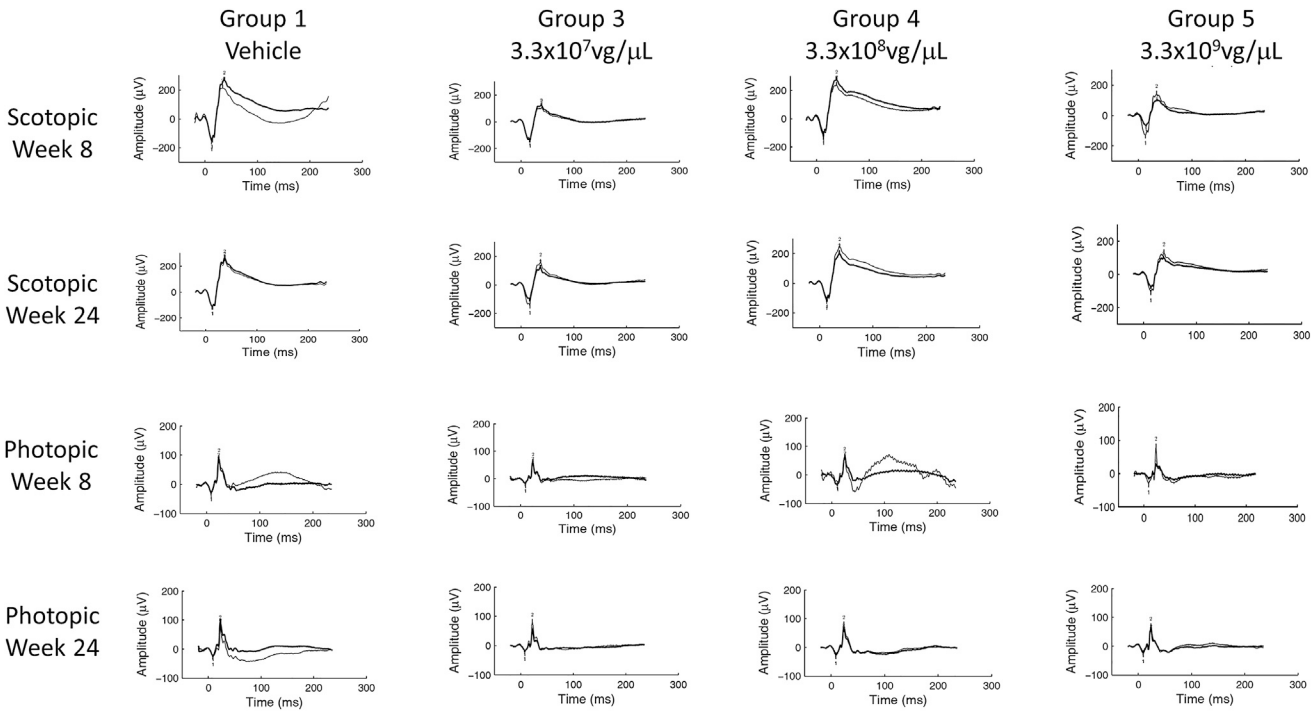

Figure 5. Representative ERG Traces from Animals in the NHP Toxicology Study

Bold traces are the right, dosed eye; thin traces are the undosed, left eye. All animals here were left undosed in the contralateral eye at the day 51 time point. A mild reduction in ERG amplitudes for both scotopic and photopic assessments were noted.

the neural retina into the subretinal space, resulting in a subretinal bleb. On day 51 of the study, a subset of animals received an injection of 3.3×10^7 vg/µL into the right eye. Slit lamp biomicroscopy, indirect ophthalmoscopy, and intraocular pressure measurement was performed on days 3, 8, 15, 22, and 29 during week 7, days 50 (prior to dosing the right eye in a subset of animals), 52, 57, and approximately weekly thereafter until sacrifice. OCT imaging was performed once during the pre-dose phase and during weeks 1, 5, 9, 13, 17, 21, and 25 using a Heidelberg Spectralis HRA + OCT. ERG was performed during weeks 4, 8, 12, 16, 20, and 24. Ocular inflammation was quantified for aqueous flare, aqueous cells, vitreous cells, and conjunctival hyperemia in the non-human primate study by applying a score between 0–4 for no findings (0), trace findings (0.5), slight findings (1), mild findings (2), moderate findings (3), and severe findings (4). These values were added together to generate overall ocular inflammation scores.

For rat biodistribution studies, the protocol was approved by the Covance Institutional Animal Care and Use Committee, and the study was conducted in compliance with all regulatory requirements. A blunt-tipped needle (33- gauge) was inserted tangentially through the scleral incision toward the back of the eye, avoiding the lens. The needle was advanced further to the edge of the opposite retina, and 2 µL of vehicle or test article formulation was injected as a bolus into the subretinal space, causing a focal retinal detachment. The subretinal injection was administered to the right eye only.

Anti-AAV8 and CRALBP Analysis

ELISA plates were coated with AAV8 followed by washing and blocking. Positive controls (anti-AAV8 antibodies) in non-human primate serum and samples were diluted and then added to the plate and bound the AAV8 coated to the plate. After incubation, plates were washed and conjugate was added. Following incubation with the conjugate, plates were washed and 3,3′,5,5′- tetramethylbenzidine (TMB) 2-component chromogenic substrate was added. After sufficient color development, the reaction was stopped by the addition of stop solution. The optical density (OD) of each well was determined by wavelength measurement at 450 nm, with a correction at 570 nm. Absorbance values (OD 450–570) obtained from replicate wells of each control and sample were averaged. Signal data were analyzed using SoftMax Pro GxP software.

Since pre-existing antibodies against AAV8 prevented determination of a screening cut point, samples were initially analyzed for anti-AAV8 antibodies in a confirmatory assay. Samples were considered positive whenever depletion was at or exceeded 24% when unspiked samples were compared with samples spiked with AAV8. Immunodepleted samples with a reduction in signal response of <24.0% when compared to the undepleted sample, but where the OD response was determined to be sufficiently high that the concentration of AAV8 used for depletion may have been insufficient, were diluted further and repeated in the confirmatory assay. Samples that were confirmed positive for anti-AAV8 antibodies were subsequently

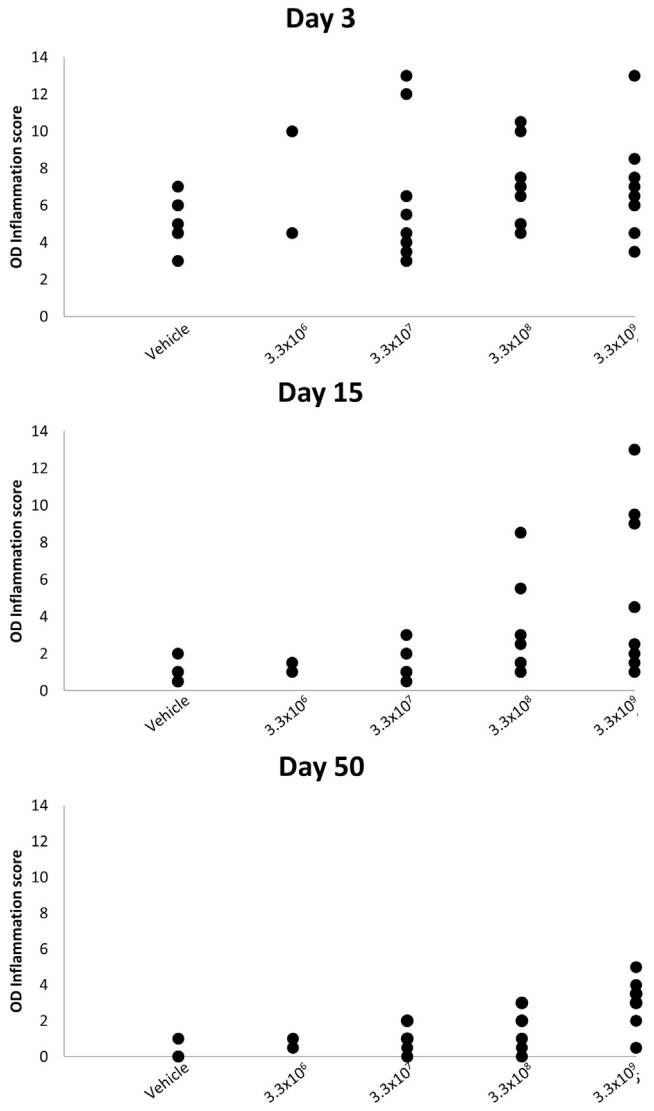

Figure 6. Composite Inflammation Scores from Animals in the Non-human Primate Toxicology Study

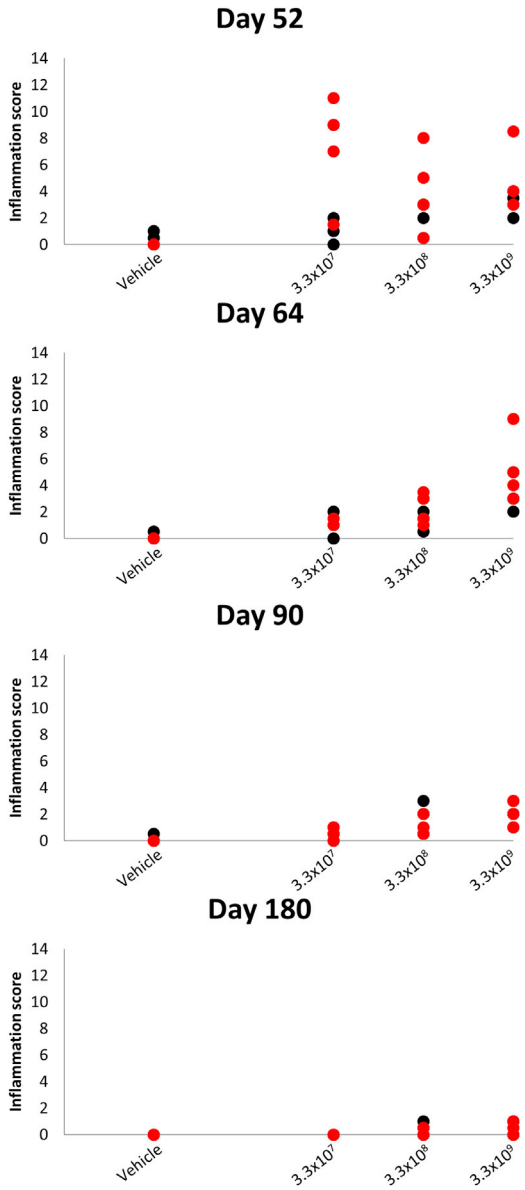

Figure 7. Composite Inflammation Scores from the Subset of Non-human Primates Also Dosed in the Right Eye on Day 50

Left eyes are displayed in black and right eyes in red.

titered to estimate the level of antibody. As a screening cut point was not established, 2 × the OD for the plate NC (negative control) was utilized as the titer cut point. The titer was defined as the reciprocal of the highest dilution, which resulted in a response above the titer cut point. Only 4 dilution steps were used to maximize the throughput. Samples with titers above 1,024 were not reanalyzed at further dilution and were reported as >1,024.

The titers of pre-existing anti-AAV8 antibodies ranged from 0 to 256. The presence of pre-existing antibodies can present challenges in the interpretation of immunogenicity data after the administration of gene therapies. It is not possible to easily categorize a response as being treatment-induced (i.e., no anti-vector antibodies detected pre-dose with anti-vector antibodies detected post-dose) or treatment-boosted (i.e., anti-vector antibodies detected pre-dose with an increase in antibody titer post-dose) due to the inherent fluctuation in antibody titers or a potential concomitant infection with the parental virus. This inherent variability is apparent in the data generated from the control group animals. In this group there were some animals in which anti-AAV8 antibodies were not detected at any time point, some animals in which pre-existing anti-AAV8 were detected and the titer increased after vehicle administration, and some animals in which pre-existing anti-AAV8 were detected and the titer decreased after administration of the vehicle. Due to the high

Table 5. Anti-AAV8 Titers in the Non-human Primate Toxicology Study

	Study Day								
	−20	−13	15	22	50	78	114	142	177
Vehicle	128	64	64	16	32	32	16	16	4
	16	16	16	8	4	64	32	16	8
	2	2	2	2	8	4	16	4	2
	4	4	4	4	32	16	8	8	8
	0	0	0	0	0	0	0	0	0
	16	4	4	4	2	2	2	2	2
	4	2	1	2	1	1	0	1	0
	0	0	0	0	0	0	0	0	0
3.3×10^6	32	16	64	8	16	32	[a]	[a]	[a]
	2	64	8	8	4	2	[a]	[a]	[a]
3.3×10^7	2	2	512	512	512	0	128	64	64
	1	0	<1	<1	<1	0	0	0	<1
	0	0	16	8	1	<1	[a]	[a]	[a]
	8	8	512	256	64	1,024[b]	256[b]	128[b]	64[b]
	8	8	256	256	64	128[b]	128[b]	128[b]	64[b]
	4	4	4	8	4	4	4	4	2
	4	4	8	8	4	4	4	2	8
	1	<1	1	1	1	<1	[a]	[a]	[a]
	4	4	1,024	1,024	512	1,024[b]	256[b]	128[b]	128[b]
	1	1	4	4	32	128[b]	128[b]	32[b]	64[b]
3.3×10^8	4	4	512	256	64	16	16	16	16
	64	32	256	512	256	256	64	32	32
	4	4	64	128	256	512	[a]	[a]	[a]
	16	8	128	256	128	256[b]	128[b]	128[b]	128[b]
	1	1	16	32	64	128[b]	64[b]	64[b]	32[b]
	256	128	128	256	256	256	256	128	128
	8	4	128	64	256	256	256	256	256
	8	8	128	256	128	256	[a]	[a]	[a]
	16	16	1,024	1,024	1,024	512[b]	512[b]	256[b]	256[b]
	128	256	512	512	512	512[b]	512[b]	512[b]	512[b]
3.3×10^9	0	0	1,024	128	128	64	64	64	128
	0	0	16	64	64	32	32	32	64
	0	1	1,024	IS	512	512	[a]	[a]	[a]
	8	64	256	1,024	512	256[b]	128[b]	128[b]	128[b]
	0	0	128	128	256	512[b]	128[b]	128[b]	64[b]
	0	0	16	128	128	256	256	128	64
	16	8	64	256	128	64	32	32	32
	8	8	512	1,024	1,024	1,024	[a]	[a]	[a]
	2	2	64	128	512	1,024[b]	1,024[b]	512[b]	512[b]
	0	0	16	16	256	512[b]	512[b]	256[b]	256[b]

Numbers indicate titer of antibody, i.e., the dilution of neat serum where signal is no longer detectable. IS, insufficient sample.
[a]Animals were sacrificed at the 3-month time point for expression and histology analysis.
[b]Animals were dosed with 3.3×10^7 vg/μL in the right eye on day 51.

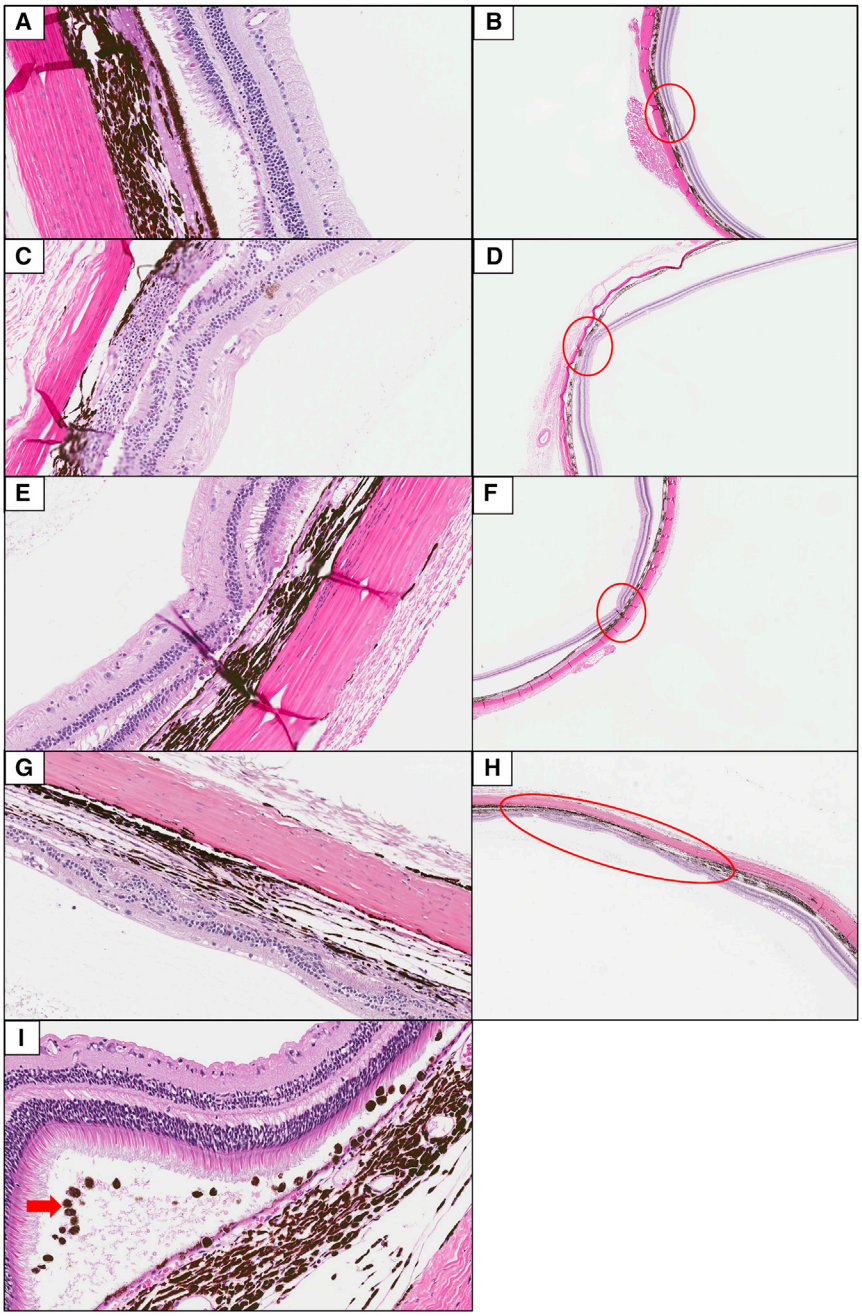

Figure 8. Representative Photomicrographs of Retinal Atrophy (Thinning, Extent Indicated by Red Circles) and Choroidal Mononuclear Cell Infiltrates and Pigmented Cells Observed in the Non-human Primate Toxicology Study

Animals from the vehicle control (A and B), 3.3×10^7 (C and D) and 3.3×10^8 (E and F) vg/μL dose groups showing minimal to mild focal atrophy and/or degeneration at the 6-month sacrifice, and an animal at the 3.3×10^9 vg/μL dose group 6 months post-injection showing moderate, locally extensive degeneration (G and H). Mild level of mononuclear and pigmented cell infiltration (red arrow) in the 3.3×10^9 vg/μL dose group 3 months post-injection (I). Original magnification, 40× (A, C, E, and G); original magnification, 4× (B, D, F, and H); original magnification, 20× (I) H&E.

incidence of anti-AAV8 antibodies, ~90% of the samples were confirmed positive and analyzed in the titer assay (4 dilutions). More than 150 samples had to be repeated at higher dilutions.

For anti-CRALBP antibodies, streptavidin-coated plates were blocked while simultaneously incubating controls and samples with a mixture of Biotin labeled CRALBP and Sulfo-Tag labeled CRALBP. After incubation, the sample mixture was added to the blocked streptavidin-coated plate, and the plates were then incubated on a plate shaker at room temperature (RT). The plates were washed and read buffer was added immediately, followed by reading of the plates. The signal data were captured on an MSD Sector Imager 6000 and analyzed using SoftMax Pro GxP software.

Biodistribution and Expression Analysis

In the rat, a comprehensive tissue set was collected at the three sacrifice time points as outlined in Tables 6 and 7. In addition, on day 15, nasopharyngeal swabs, urine, and feces were collected for shedding analysis. After preparation for DNA, samples were assessed for CPK850 DNA by PCR. In the non-human primate, an assessment of the tissue distribution and the excretion of CPK850 was performed in the subset of animals that were sacrificed at the 3-month time point (one male and one female in groups 2–5). Tear samples (from left and right eyes), throat swabs, and urine and fecal swabs were collected from this group of animals during weeks 1, 4, 8, and 12 post-dose. Lacrimal gland and brain samples (including optic chiasm, optic tract, lateral geniculate nucleus, visual cortex, and superior colliculus) were collected at necropsy, processed to DNA, and analyzed for the presence of CPK850. A TaqMan qPCR assay using the probes listed below was employed to detect and quantify the presence of vector DNA sequence in shedding samples and tissues.

Forward: 5′-AGC AAT AGC ATC ACA AAT TTC ACA A-3′

Reverse: 5′-CCA GAC ATG ATA AGA TAC ATT GAT GAG TT-3′

Probe: 5′-AGC ATT TTT TTC ACT GCA TTC TAG TTG TGG TTT GTC-3′

Table 6. Design of Rat Biodistribution Study

	Animals		Dose Concentration (vg/μL)[a]	
Group	Male	Female	Right Eye	Left Eye
1[b]	5	5	0 (vehicle)	NA
2[c]	15	15	3.3×10^7	NA

[a]Dose volume per eye was 2 μL.
[b]Group was sacrificed on study day 15.
[c]5 males and 5 females in this group were sacrificed on study days 15, 57, and 85.

Table 7. Tissues Collected in Rat Distribution Study

Males	Females
Brain[a]	brain[a]
Left eye (undosed)	left eye (undosed)
Right eye (dosed)	right eye (dosed)
Optic nerve[b]	optic nerve[b]
Testes[b]	ovaries[b]
	mandibular lymph node[b]
	salivary gland[b]
	skeletal muscle (cranial)
	liver
	spleen
	lungs[b]
	kidneys[b]
	jejunum
	heart

[a]A sample was collected separately from the left and right side of the brain.
[b]Each sample was collected separately as left and right.

Additionally, from the non-human primate sacrificed at 3 months, eyes were collected and sectioned as shown in Figure 4 for evaluation of expression of human *RLBP1* transcript. Samples were prepared for RNA and evaluated by an RT-PCR assay that can differentiate between the non-human primate and human *RLBP1* transcripts.

ERG in *Rlbp1*$^{-/-}$ and *Rlbp1*$^{+/+}$ Mice

For mouse safety studies, ERG was performed 10 to 11 weeks post-injection. This allowed indirect confirmation of vector-mediated CRALBP expression in *Rlbp1*$^{-/-}$ mouse eyes through detection of an increased dark adaptation rate. Equivalent confirmation of vector-mediated CRALBP expression in *Rlbp1*$^{+/+}$ mice was not possible due to endogenous protein expression, although assessment of qualitative visual function was provided by ERG. For the dose-response efficacy study, recordings occurred 12 weeks post-injection.

ERG was performed in two sessions for each study, with ERG recorded from one eye per mouse. In one session, the baseline maximum dark-adapted response of each eye to light was determined. Mice were first housed in the dark overnight in a ventilated, light-tight enclosure (Phenome Technologies, Chicago, IL). Prior to recording, pupils were dilated with one or two drops of 1% cyclopentolate and one or two drops of 2.5% or 10% phenylephrine. Anesthesia was provided by an intraperitoneal injection of a ketamine/xylazine cocktail (100–150/5–10 mg/kg), and topical 0.5% proparacaine was applied to the eyes. Body temperature was maintained by placing mice on a warm water heating pad. ERG traces were recorded using a gold loop contact lens electrode (N30, LKC Technologies, Gaithersburg, MD) referenced to a gold nasopharyngeal electrode placed in the mouth (F-ERG-G, Grass Technologies, Warwick, RI). Stable ocular hydration was accomplished through continuous application of 0.3% hypromellose drops (GenTeal, Alcon, Fort Worth, TX) through flexible tubing at 300 μL/hr. Electrical ground was provided by a 30-gauge platinum subdermal needle electrode placed near the scapular region (F-E2, Grass Technologies). Photoreceptor responses were quantified through ERG a-wave amplitude measured 5 ms after a 2.7 log scotopic (scot) cd s m^{-2} white light flash from a xenon bulb; up to 3 successive flashes were averaged, with traces containing artifacts excluded prior to averaging. Extraction of amplitudes was accomplished using a script written for this purpose in MATLAB (Mathworks, Natick, MA). Dark adaptation was assessed by first housing the mice overnight in the dark. Photopigment was bleached by exposing each eye to a series of 16 flashes of light (3.7 log scot cd s m^{-2} white light flash from a xenon bulb) while mice were conscious and after pupil dilation with cyclopentolate and phenylephrine. ERG a-wave response was subsequently determined 4 hours later using the same procedure as the baseline measurement. a-wave recovery achieved in 4 hr post-bleach relative to the maximum dark-adapted amplitude was calculated for each eye. Eyes that recovered complete visual function in 4 hr yielded recoveries approaching 100%. All recordings were performed with a commercial ERG system (Diagnosys Espion E2 with dual ColorDome Ganzfeld domes, Diagnosys, Lowell, MA). Statistical analysis was performed using a one-way ANOVA with Tukey's multiple comparison test.

Imaging and Histology of the Retina in the *Rlbp1*$^{-/-}$ and *Rlbp1*$^{+/+}$ Mouse Study

Images of the mouse retina were acquired using an OCT system (Bioptigen, Morrisville, NC) to generate volumetric scans centered on the optic nerve as much as feasible. Images were acquired prior to injection, approximately 1 week post-injection, and approximately 12 weeks post-injection. Images acquired 1 week post-injection were used as a screen of injection quality. Eyes demonstrating unacceptable complications from the injection procedure (e.g., unresolved retinal detachments, large hemorrhages, or excessive retinal structure damage) were excluded from additional assessment at 12 weeks. Images captured 12 weeks post-injection were used to determine the effects of the delivery of vehicle or CPK850 on the mouse eye. Pre-injection images were used as a reference to identify if observations noted in the 12-week OCT images were pre-existing and therefore not attributable to vehicle or CPK850.

Findings from each OCT image were assigned to one of six categories as described in Table S1. Representative images of these categories are provided in Figure S1. Two graders reviewed the images of the eyes in

Table 8. Biodistribution Shedding Analyses: Results of the Rat Biodistribution Study

	No. of Animals with Detectable CPK850			Median Copies of CPK850/μg DNA		
Tissue	Day 15	Day 57	Day 85	Day 15	Day 57	Day 85
Eye (L)	7/10	7/10	2/10	112	61	<50
Eye (R)	9/10	10/10	9/10	>1,000,000	677,000	>1,000,000
Optic nerve (L)	1/10	2/10	1/10	<50	<50	<50
Optic nerve (R)	9/10	7/10	9/10	5,570	2,260	191
Brain (L)	6/10	0/10	0/10	278	<50	<50
Brain (R)	1/10	0/10	0/10	<50	<50	<50
Mandibular lymph node (L)	3/5	3/5	3/5	160	87	59
Mandibular lymph node (R)	4/5	5/5	2/5	347	172	<50
Salivary gland (L)	0/5	0/5	0/5	<50	<50	<50
Salivary gland (R)	0/5	0/5	0/5	<50	<50	<50
Lung (L)	0/5	1/5	0/5	<50	<50	<50
Lung (R)	1/5	0/5	0/5	<50	<50	<50
Skeletal muscle	1/5	0/5	0/5	<50	<50	<50
Spleen	5/5	5/5	5/5	3,540	467	696
Heart (atria)	0/5	0/5	0/5	<50	<50	<50
Heart (ventricle)	0/5	0/5	0/5	<50	<50	<50
Jejunum	0/5	0/5	0/5	<50	<50	<50
Kidney (L)	1/5	0/5	0/5	<50	<50	<50
Kidney (R)	1/5	0/5	0/5	<50	<50	<50
Liver	4/5	5/5	2/5	211	226	<50
Ovary (L)	0/5	0/5	0/5	<50	<50	<50
Ovary (R)	0/5	0/5	0/5	<50	<50	<50
Testes (L)	0/5	0/5	0/5	<50	<50	<50
Testes (R)	0/5	0/5	0/5	<50	<50	<50

Numbers indicate copy number of DNA detected. The level of quantification in the assay was 50 copies per microgram of genomic DNA and the level of detection was 10 copies per microgram of DNA. L, left; R, right.

a masked and randomized fashion to assign each eye to one of the categories. If an eye exhibited features consistent with more than one category, the eye was assigned to the category interpreted as representing more significant pathology.

A qualitative estimate of the degree of retinal thinning was also generated to provide a graphical representation of this aspect of retinal structure. During review of the 12-week post-injection OCT images, two estimates were generated from visual inspection of volumetric OCT scans. The first estimate was of the fraction of the scan that exhibited retinal thinning (area of coverage). The second estimate was of the average fraction of the retina observed to be lost within the region exhibiting thinning (amount of thinning). In eyes that did not exhibit thinning, both estimates were zero. A composite metric termed "estimated retinal thickness" was generated by first multiplying the area of coverage by the amount of thinning to yield Y, and then further scaling Y according to

$$\text{estimated retinal thickness} = \left(1 - \left(\frac{Y}{10,000}\right)\right) \times 100.$$

The result of this scaling is that a normal retina would result in a value of 100, while a scan with no visible neural retina would result in a value of 0.

For histopathological evaluation, eyes were enucleated at the time of necropsy and immediately placed in >3 mL per eye of Davidson's fixative, where eyes were fixed for 24–48 hr at RT. Eyes were then gently rinsed and stored in 10% neutral-buffered formalin. The eyes were left in their entirety at trimming and placed within a specific area of sponge to maintain their orientation. Eyes from one animal were placed in one cassette, with the left eye being set closest to the slide label. They were processed overnight and embedded maintaining left and right orientation. The eyes were sectioned 500 μm apart, resulting in 5 levels per eye, 10 sections per animal in total. They were then stained with H&E and reviewed by light microscopy.

After microscopic review of the tissue from each of the 5 levels, a mean grade was assigned to any observed lesion using the subjective grading scheme of normal, minimal, mild, moderate, and marked.

Table 9. Biodistribution Shedding Analyses: Results of Distribution in the Non-human Primate Eye and Brain Biodistribution Study

Dose Group	Copies of CPK850 Detected/μg DNA												
	Right Lacrimal Gland	Left Lacrimal Gland	Right Optic Nerve	Left Optic Nerve	Right Optic Chiasm	Left Optic Chiasm	Right Optic Tract	Left Optic Tract	Right Lateral Geniculate Nucleus	Left Lateral Geniculate Nucleus	Right Superior Colliculus	Left Superior Colliculus	Right Visual Cortex	Left Visual Cortex
3.3×10^6 #1	–	–	–	–	–	–	–	–	–	–	–	–	–	–
3.3×10^6 #2	–	–	–	–	–	–	–	–	–	–	–	–	–	–
3.3×10^7 #1	720	–	1,015	–	636	–	188	142	–	–	–	–	–	–
3.3×10^7 #2	–	–	765	–	202	–	82	191	–	–	–	–	–	–
3.3×10^8 #1	–	–	22,743	–	9,068	1,747	2,272	1,176	–	–	–	300	–	–
3.3×10^8 #2	–	–	197	–	–	128	–	67	–	–	–	–	–	–
3.3×10^9 #1	36,110	389	37,401	–	11,461	359	7,551	612	–	–	269	157	–	–
3.3×10^9 #2	–	–	10,881	–	1,638	220	371	688	83	294	–	81	–	–

Numbers indicate copy number of DNA detected. The level of quantification in the assay was 50 copies per microgram of genomic DNA, and the level of detection was 10 copies per microgram of DNA. Dashes indicate results were below the limit of quantitation.

Table 10. Biodistribution Shedding Analyses: Results of Shedding Sample Analysis from Non-human Primates

		Copies of CPK850 Detected			
	Dose Group	Week 1	Week 4	Week 8	Week 12
Tears[a]	3.3×10^6 #1	–	–	–	–
	3.3×10^6 #2	–	–	–	–
	3.3×10^7 #1	–	–	–	–
	3.3×10^7 #2	–	–	–	–
	3.3×10^8 #1	–	–	9,464	–
	3.3×10^8 #2	–	–	–	–
	3.3×10^9 #1	–	–	138	104
	3.3×10^9 #2	1,881	–	–	–
Throat swabs	3.3×10^6 #1	134	–	–	–
	3.3×10^6 #2	–	–	–	–
	3.3×10^7 #1	–	–	–	–
	3.3×10^7 #2	–	–	–	–
	3.3×10^8 #1	60	–	–	–
	3.3×10^8 #2	–	–	–	–
	3.3×10^9 #1	–	–	–	–
	3.3×10^9 #2	146	–	–	–
Urine	3.3×10^6 #1	–	–	–	–
	3.3×10^6 #2	–	–	–	–
	3.3×10^7 #1	–	–	–	–
	3.3×10^7 #2	–	–	–	–
	3.3×10^8 #1	–	–	–	–
	3.3×10^8 #2	–	–	–	–
	3.3×10^9 #1	–	–	–	–
	3.3×10^9 #2	3	–	–	–
Fecal swabs	3.3×10^6 #1	–	–	–	–
	3.3×10^6 #2	–	–	–	–
	3.3×10^7 #1	–	–	–	–
	3.3×10^7 #2	–	–	–	–
	3.3×10^8 #1	–	–	–	–
	3.3×10^8 #2	133	–	–	–
	3.3×10^9 #1	199	–	–	–
	3.3×10^9 #2	142	–	–	–

Numbers indicate copy number of DNA detected. The level of quantification in the assay was 50 copies per microgram of genomic DNA, and the level of detection was 10 copies per microgram of DNA. Dashes indicate results were below the limit of quantitation.

[a]Tears from the right and left eyes were combined.

The criteria for each grade for the lesion of atrophy (thinning) of the outer retina are described in Table S2.

Histology of the Retina in the Non-human Primate Study

At the 3 months interim sacrifice, a rectangular section of retina, including the optic disc and fovea, was sampled from a small subset of animals (Figure 4). This was immediately placed in modified

Davidson's fixative for 24–48 hr at RT and then stored in 10% neutral-buffered formalin. At the 6-month terminal sacrifice, for histopathological evaluation, eyes were enucleated at the time of harvest and immediately placed in modified Davidson's fixative for 24–48 hr at RT and then stored in 10% neutral-buffered formalin. Eyes with bulbar conjunctiva from all animals were sectioned to allow for 11 superior-inferior sections through each eye to be evaluated, which included the fovea.

After microscopic review of the tissue from each of the 11 levels, a mean grade was assigned to any observed lesion using the subjective grading scheme of normal, minimal (focal), mild (focal or multifocal), and moderate (locally extensive to multifocal).

SUPPLEMENTAL INFORMATION

Supplemental Information includes two figures and two tables and can be found with this article online at https://doi.org/10.1016/j.omtm.2017.12.001.

AUTHOR CONTRIBUTIONS

T.K.M. led the conduct and strategy of the nonclinical safety program and wrote this manuscript; M.N.M. led the conduct and strategy of the biodistribution studies; O.T. conducted pathology analysis on the mouse and primate studies; C.E.B. conducted mouse efficacy studies and mouse safety studies; F.T. monitored the primate safety studies; V.W.C. conducted the initial mouse efficacy studies and mouse safety studies; J.P. conducted the OCT analyses in the mouse studies; M.-H.D. evaluated the data from the PCR analysis in the biodistribution studies; L.M. evaluated the data from the immunogenicity samples in the primate study; B.D.J. oversaw the strategy of the mouse and monkey studies.

ACKNOWLEDGMENTS

The authors thank Stephen Poor for performing rat subretinal injections; Joanna Vrouvlianis, Shawn Hanks, Barrett Leehy, and Michael Maker for *in vivo* ocular assessments in mouse studies; Akshata Gujar and Jorge Aranda for viral vector delivery procedures in mouse studies; and Hui Li for subretinal injections in mice.

REFERENCES

1. Choi, V.W., Bigelow, C.E., McGee, T.L., Gujar, A.N., Li, H., Hanks, S.M., Vrouvlianis, J., Maker, M., Leehy, B., Zhang, Y., et al. (2015). AAV-mediated RLBP1 gene therapy improves the rate of dark adaptation in Rlbp1 knockout mice. Mol. Ther. Methods Clin. Dev. *2*, 15022.
2. Daiger, S.P., Sullivan, L.S., and Bowne, S.J. (2013). Genes and mutations causing retinitis pigmentosa. Clin. Genet. *84*, 132–141.
3. Maw, M.A., Kennedy, B., Knight, A., Bridges, R., Roth, K.E., Mani, E.J., Mukkadan, J.K., Nancarrow, D., Crabb, J.W., and Denton, M.J. (1997). Mutation of the gene encoding cellular retinaldehyde-binding protein in autosomal recessive retinitis pigmentosa. Nat. Genet. *17*, 198–200.
4. Eichers, E.R., Green, J.S., Stockton, D.W., Jackman, C.S., Whelan, J., McNamara, J.A., Johnson, G.J., Lupski, J.R., and Katsanis, N. (2002). Newfoundland rod-cone dystrophy, an early-onset retinal dystrophy, is caused by splice-junction mutations in RLBP1. Am. J. Hum. Genet. *70*, 955–964.
5. Golovleva, I., Bhattacharya, S., Wu, Z., Shaw, N., Yang, Y., Andrabi, K., West, K.A., Burstedt, M.S., Forsman, K., Holmgren, G., et al. (2003). Disease-causing mutations in the cellular retinaldehyde binding protein tighten and abolish ligand interactions. J. Biol. Chem. *278*, 12397–12402.
6. He, X., Lobsiger, J., and Stocker, A. (2009). Bothnia dystrophy is caused by domino-like rearrangements in cellular retinaldehyde-binding protein mutant R234W. Proc. Natl. Acad. Sci. USA *106*, 18545–18550.
7. Travis, G.H., Golczak, M., Moise, A.R., and Palczewski, K. (2007). Diseases caused by defects in the visual cycle: retinoids as potential therapeutic agents. Annu. Rev. Pharmacol. Toxicol. *47*, 469–512.
8. Wang, J.S., and Kefalov, V.J. (2009). An alternative pathway mediates the mouse and human cone visual cycle. Curr. Biol. *19*, 1665–1669.
9. Wang, J.S., and Kefalov, V.J. (2011). The cone-specific visual cycle. Prog. Retin. Eye Res. *30*, 115–128.
10. Jacobson, S.G., Boye, S.L., Aleman, T.S., Conlon, T.J., Zeiss, C.J., Roman, A.J., Cideciyan, A.V., Schwartz, S.B., Komaromy, A.M., Doobrajh, M., et al. (2006). Safety in nonhuman primates of ocular AAV2-RPE65, a candidate treatment for blindness in Leber congenital amaurosis. Hum. Gene Ther. *17*, 845–858.
11. Jacobson, S.G., Acland, G.M., Aguirre, G.D., Aleman, T.S., Schwartz, S.B., Cideciyan, A.V., Zeiss, C.J., Komaromy, A.M., Kaushal, S., Roman, A.J., et al. (2006). Safety of recombinant adeno-associated virus type 2-RPE65 vector delivered by ocular subretinal injection. Mol. Ther. *13*, 1074–1084.
12. Cideciyan, A.V., Hauswirth, W.W., Aleman, T.S., Kaushal, S., Schwartz, S.B., Boye, S.L., Windsor, E.A., Conlon, T.J., Sumaroka, A., Pang, J.J., et al. (2009). Human RPE65 gene therapy for Leber congenital amaurosis: persistence of early visual improvements and safety at 1 year. Hum. Gene Ther. *20*, 999–1004.
13. Maguire, A.M., Simonelli, F., Pierce, E.A., Pugh, E.N., Jr., Mingozzi, F., Bennicelli, J., Banfi, S., Marshall, K.A., Testa, F., Surace, E.M., et al. (2008). Safety and efficacy of gene transfer for Leber's congenital amaurosis. N. Engl. J. Med. *358*, 2240–2248.
14. Bainbridge, J.W., Mehat, M.S., Sundaram, V., Robbie, S.J., Barker, S.E., Ripamonti, C., Georgiadis, A., Mowat, F.M., Beattie, S.G., Gardner, P.J., et al. (2015). Long-term effect of gene therapy on Leber's congenital amaurosis. N. Engl. J. Med. *372*, 1887–1897.
15. Amado, D., Mingozzi, F., Hui, D., Bennicelli, J.L., Wei, Z., Chen, Y., Bote, E., Grant, R.L., Golden, J.A., Narfstrom, K., et al. (2010). Safety and efficacy of subretinal readministration of a viral vector in large animals to treat congenital blindness. Sci. Transl. Med. *2*, 21ra16.
16. Bennett, J., Ashtari, M., Wellman, J., Marshall, K.A., Cyckowski, L.L., Chung, D.C., McCague, S., Pierce, E.A., Chen, Y., Bennicelli, J.L., et al. (2012). AAV2 gene therapy readministration in three adults with congenital blindness. Sci. Transl. Med. *4*, 120ra15.
17. Bennett, J., Wellman, J., Marshall, K.A., McCague, S., Ashtari, M., DiStefano-Pappas, J., Elci, O.U., Chung, D.C., Sun, J., Wright, J.F., et al. (2016). Safety and durability of effect of contralateral-eye administration of AAV2 gene therapy in patients with childhood-onset blindness caused by RPE65 mutations: a follow-on phase 1 trial. Lancet *388*, 661–672.
18. Bennicelli, J., Wright, J.F., Komaromy, A., Jacobs, J.B., Hauck, B., Zelenaia, O., Mingozzi, F., Hui, D., Chung, D., Rex, T.S., et al. (2008). Reversal of blindness in animal models of leber congenital amaurosis using optimized AAV2-mediated gene transfer. Mol. Ther. *16*, 458–465.
19. Fischer, M.D., Hickey, D.G., Singh, M.S., and MacLaren, R.E. (2016). Evaluation of an Optimized Injection System for Retinal Gene Therapy in Human Patients. Hum. Gene Ther. Methods *27*, 150–158.
20. Nork, T.M., Murphy, C.J., Kim, C.B., Ver Hoeve, J.N., Rasmussen, C.A., Miller, P.E., Wabers, H.D., Neider, M.W., Dubielzig, R.R., McCulloh, R.J., and Christian, B.J. (2012). Functional and anatomic consequences of subretinal dosing in the cynomolgus macaque. Arch. Ophthalmol. *130*, 65–75.
21. Ramachandran, P.S., Lee, V., Wei, Z., Song, J.Y., Casal, G., Cronin, T., Willett, K., Huckfeldt, R., Morgan, J.I., Aleman, T.S., et al. (2017). Evaluation of Dose and Safety of AAV7m8 and AAV8BP2 in the Non-Human Primate Retina. Hum. Gene Ther. *28*, 154–167.
22. Ye, G.J., Budzynski, E., Sonnentag, P., Nork, T.M., Miller, P.E., Sharma, A.K., Ver Hoeve, J.N., Smith, L.M., Arndt, T., Calcedo, R., et al. (2016). Safety and Biodistribution Evaluation in Cynomolgus Macaques of rAAV2tYF-PR1.7-hCNGB3, a Recombinant AAV Vector for Treatment of Achromatopsia. Hum. Gene Ther. Clin. Dev. *27*, 37–48.

23. Ye, G.J., Budzynski, E., Sonnentag, P., Nork, T.M., Miller, P.E., McPherson, L., Ver Hoeve, J.N., Smith, L.M., Arndt, T., Mandapati, S., et al. (2016). Safety and Biodistribution Evaluation in CNGB3-Deficient Mice of rAAV2tYF-PR1.7-hCNGB3, a Recombinant AAV Vector for Treatment of Achromatopsia. Hum. Gene Ther. Clin. Dev. *27*, 27–36.

24. Deng, W.T., Dyka, F.M., Dinculescu, A., Li, J., Zhu, P., Chiodo, V.A., Boye, S.L., Conlon, T.J., Erger, K., Cossette, T., and Hauswirth, W.W. (2015). Stability and Safety of an AAV Vector for Treating RPGR-ORF15 X-Linked Retinitis Pigmentosa. Hum. Gene Ther. *26*, 593–602.

25. Binley, K., Widdowson, P.S., Kelleher, M., de Belin, J., Loader, J., Ferrige, G., Carlucci, M., Esapa, M., Chipchase, D., Angell-Manning, D., et al. (2012). Safety and biodistribution of an equine infectious anemia virus-based gene therapy, RetinoStat(®), for age-related macular degeneration. Hum. Gene Ther. *23*, 980–991.

26. Tan, E., Wang, Q., Quiambao, A.B., Xu, X., Qtaishat, N.M., Peachey, N.S., Lem, J., Fliesler, S.J., Pepperberg, D.R., Naash, M.I., and Al-Ubaidi, M.R. (2001). The relationship between opsin overexpression and photoreceptor degeneration. Invest. Ophthalmol. Vis. Sci. *42*, 589–600.

27. Wenzel, A., Reme, C.E., Williams, T.P., Hafezi, F., and Grimm, C. (2001). The Rpe65 Leu450Met variation increases retinal resistance against light-induced degeneration by slowing rhodopsin regeneration. J. Neurosci. *21*, 53–58.

28. Mehalow, A.K., Kameya, S., Smith, R.S., Hawes, N.L., Denegre, J.M., Young, J.A., Bechtold, L., Haider, N.B., Tepass, U., Heckenlively, J.R., et al. (2003). CRB1 is essential for external limiting membrane integrity and photoreceptor morphogenesis in the mammalian retina. Hum. Mol. Genet. *12*, 2179–2189.